MAGNESIUM RECYCLING OF PARTIALLY OXIDIZED, MIXED MAGNESIUM-ALUMINUM SCRAP THROUGH COMBINED REFINING AND SOLID OXIDE MEMBRANE (SOM) ELECTROLYSIS PROCESSES

Xiaofei Guan[1], Peter Zink[1,2], Uday Pal[1,2]

[1]Boston University, Division of Materials Science and Engineering; 15 Saint Mary's St.; Brookline, MA, 02446
[2]Boston University, Department of Mechanical Engineering; 110 Cummington St.; Boston, MA, 02215

Keywords: Magnesium, Refining, SOM Electrolysis

Abstract

Pure magnesium (Mg) is recycled from 19g of partially oxidized 50.5wt.%Mg-Aluminum (Al) alloy. During the refining process, potentiodynamic scans (PDS) were performed to determine the electrorefining potential for magnesium. The PDS show that the electrorefining potential increases over time as the Mg content inside the Mg-Al scrap decreases. Up to 100% percent of magnesium is refined from the Mg-Al scrap by a novel refining process of dissolving magnesium and its oxide into a flux followed by vapor phase removal of dissolved magnesium and subsequently condensing the magnesium vapors in a separate condenser. The solid oxide membrane (SOM) electrolysis process is employed in the refining system to enable additional recycling of magnesium from magnesium oxide (MgO) in the partially oxidized Mg-Al scrap. The combination of the refining and SOM processes yields 7.4g of pure magnesium; could not collect and weigh all of the magnesium recovered.

Introduction

Magnesium is the least dense engineering metal, with an excellent stiffness-to-weight ratio. For this reason, U.S. auto makers would like to replace 630 lb. of steel and aluminum parts per vehicle with 340 lb. of magnesium alloy by the year 2020 [1]. This would reduce vehicle weight by 290 lbs and improve average fuel efficiency by 1.5-2 miles per gallon, reducing petroleum imports by up to 1 million barrels per day. Additionally, the fact that magnesium has good electromagnetic shielding makes it very attractive to the audio and electronic industry [2]. As magnesium consumption increases in the automotive, aerospace and electronic industries, magnesium recycling will become ever more important for both economic and environmental reasons.

Several recycling processes are currently in use. Some are based on the use of refining fluxes, and others are flux-free methods. Hydro Magnesium [3, 4] has a system for continuous melting with flux. Magnesium alloy is melted in one end of a large multi-chamber furnace and pumped out or cast from the other end. This refining process uses sufficient flux to absorb all the oxides present in the molten metal, but it cannot separate pure magnesium from aluminum and trace impurities such as zinc, iron and nickel; impurities like nickel and iron decrease corrosion resistance of magnesium [5]. Zhu et al [6] demonstrated that vacuum distillation for magnesium recycling. However, the vacuum distillation will leave 20-25% of the original scrap as the residue with a magnesium weight content as high as 60%. It is understood that further magnesium distillation is hindered by the magnesium oxide and aluminum oxide (Al_2O_3) on the surface of the residue.

In this paper, an innovative process for recycling pure magnesium metal from impure magnesium scrap alloy at high efficiency and low cost is proposed. As the typical magnesium alloys in automotive components are AZ91, AM50, AM60 and so on [7], all of which are predominantly Mg-Al alloys with small amount of impurities (Zn, Mn, Fe and Ni, etc). This paper reports proof of concept experiments of our process with partially oxidized 50.5wt%Mg-Al alloy. The refining efficiency is almost 100% by dissolving magnesium and its oxide from the scrap into a flux followed by vapor phase removal of dissolved magnesium and subsequently condensing the magnesium vapors in a separate condensing chamber. After refining, the SOM electrolysis process is employed in the system to enable additional recycling of magnesium from magnesium oxide in the scrap. The combination of the refining and SOM electrolysis processes proves to be a feasible method for recycling magnesium from partially-oxidized impure magnesium scrap alloy. Future work will involve recovery of magnesium from partially oxidized magnesium scrap containing many more impurities which make it unsuitable for reuse.

Experimental

Figure 1 shows the design of the setup used in this experiment. The setup consists of an upper reaction chamber, heated to 1175°C and a lower condensing chamber with a temperature gradient of 1100-200°C. The setup was fabricated using grade 304 stainless steel (SS-304) and heated as mentioned above in an argon (Ar) atmosphere.

The Mg-Al alloy was prepared by melting a 9.6g piece of magnesium (Mg>99.8%) and another 9.4g piece of aluminum (Al>97.9%) together inside a small SS-304 crucible. The mixture of magnesium and aluminum was stirred with a SS-304 rod for 15 minutes at 800°C in an argon atmosphere, then held at the same temperature without stirring for 15 minutes and subsequently quenched. The alloy was homogeneous and the composition was 50.5wt%Mg-Al.

Since there is a finite solubility of iron in Mg-Al alloy, 2g of iron powder was added on the top of the Mg-Al alloy to decrease dissolution of iron from the crucible during the run. Also, the iron powder addition increases the density of the alloy (alloy sinks to the flux bottom in the alloy crucible) and lowers the vapor pressure of magnesium. A powdered flux (MgF_2-CaF_2-10wt.%MgO-2wt.%YF$_3$) containing a eutectic mixture of 45wt.% MgF_2-55wt.%CaF_2 with a melting point of 974°C [8] was used as the electrolyte and was packed both inside and outside the inverted crucible shown in Figure 1. In order to prevent the distillation of magnesium from the Mg-Al alloy during heating to 974°C, a layer of flux is melted on the surface of the crucible to

hermetically seal the opening of the alloy crucible before heating. Thus, the alloy is trapped inside the alloy crucibles, and the direct distillation of magnesium is avoided. A result of melting the flux at the top of alloy crucible is that some of magnesium in the alloy becomes oxidized. This magnesium oxide is later reduced with the SOM electrolysis process.

During the refining process, the alloy crucible and inverted crucible served as the anode, and the reaction chamber wall and bubbling tube served as the cathode. The SOM tube was held above the flux. An alumina spacer was used to insulate the rod connecting the inverted crucible and the reaction chamber. Potentiodynamic scans were performed to determine the electrorefining potential for magnesium, as the refining of magnesium proceeded.

During the SOM electrolysis process, an yttria stabilized zirconia (YSZ) tube was used for recycling magnesium from magnesium oxide. The stainless steel wall of the reaction chamber still served as the cathode, but silver inside the YSZ tube served as the anode, and a carbon rod acted as the anodic current collector. When the applied electric potential between the cathode and anode exceeds the dissociation potential of magnesium oxide, magnesium vapor is produced at the cathode, and carbon reacts with oxygen to generate carbon monoxide [9, 10]. The overall cell reaction is given as:

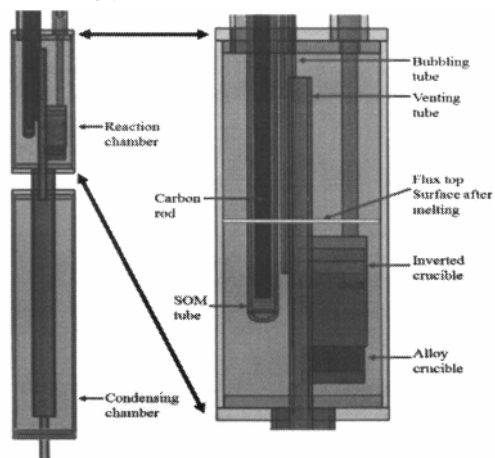$$MgO + C = Mg(g) + CO(g) \qquad (1)$$

Figure 1. Design of experimental setup for refining and SOM electrolysis processes.

It should be noted that during both the refining and electrolysis processes, the reaction chamber is continually purged with 95%Ar-H_2 at 15cc/min through a bubbling tube, and at 30cc/min through the two annuli at the top of the reaction chamber. This is done to lower the partial pressure of magnesium vapor over the flux and to carry the magnesium vapor to the condensing chamber. The inlet of the venting tube is well above the flux surface, to prevent any molten flux from entering the condenser.

Electrochemical measurements were performed. A Solartron SI 1280B potentiostat was used for potentiodynamic scans and impedance spectroscopy during the refining process; an Agilent Technologies N5743A power supply was used for potentiodynamic scans and electrolysis.

Results and Discussion

1. Refining process

Once the reaction chamber was at the desired temperature, potentiodynamic scans were performed as shown in Figure 2.The initial melted flux is entirely ionic and acts as an electronic insulator between the anode and the cathode. The current increases linearly as the applied potential increases, except at the two current jumps corresponding to magnesium dissolution and magnesium vapor formation, as can be seen in each potentiodynamic scan. The current-voltage curve is shifting in a positive direction over time from PDS1 to PDS5 due to decreasing magnesium concentration in the alloy as explained later in the paper. The ohmic resistance of the system was measured to be as low as 0.066Ω and 0.09Ω using impedance spectroscopy shown in Figure 3. One potential reason for the low resistance or the electronic conductivity is the dissolution of metallic magnesium in the flux. It has been shown that magnesium metal has some solubility in chloride based ionic salts [11]. The magnesium solubility inside the flux after the experiment was found to be 0.03wt% as measured with a manometer. Dilute acid was added to powdered flux in a closed container and the volume of gas produced due to the hydrogen evolution was measured. The flux was powdered in a glove box to avoid the oxidation of magnesium in the flux. The magnesium solubility inside a flux of similar composition (55%MgF_2-45%CaF_2-10%MgO) was reported to be 0.02-0.05wt.% [12], consistent with the experimental results .
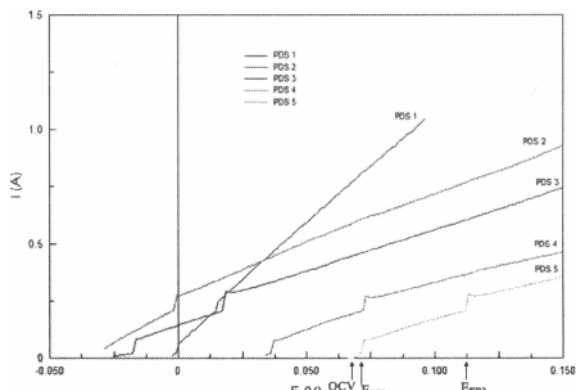

Figure 2. Potentiodynamic scans from the refining process. The open circuit voltage, two electrorefining potentials for the last potentiodynamic scan are indicated by arrows (OCV, E_{ER1}, E_{ER2}).
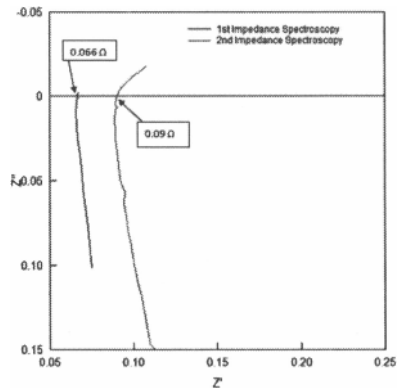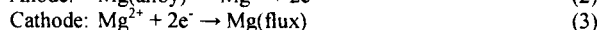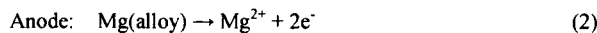

Figure 3. Impedance spectroscopy results during refining.

For each potentiodynamic scan, there are two current jumps which correspond to two different electrochemical reactions (Figure 2). The current jump at the first potential, close to the open circuit voltage is due to the following electrochemical reaction:
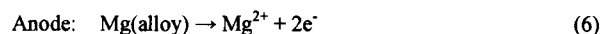
Anode: $Mg(alloy) \rightarrow Mg^{2+} + 2e^-$ (2)
Cathode: $Mg^{2+} + 2e^- \rightarrow Mg(flux)$ (3)

where the overall reaction is

$$Mg(alloy) \rightarrow Mg(flux) \qquad (4)$$

This reaction is different from direct dissolution of magnesium from Mg-Al alloy into flux. Theoretically, the first electrorefining potential corresponding to the first current jump should be equal to the open circuit voltage, and its expression is given by

$$E_{ER1} = E_{OCV} = E_{anode} - E_{cathode} = \frac{RT}{2F} \ln \frac{a_{Mg(flux)}}{a_{Mg(alloy)}} = \frac{RT}{2F} \ln \frac{P_{Mg(flux)}/P^0_{Mg}}{\gamma x_{Mg(alloy)}}$$

$$= \frac{RT}{2F} \ln \frac{P_{Mg(flux)}}{\gamma x_{Mg(alloy)} P^0_{Mg}} \qquad (5)$$

where γ is the activity coefficient of magnesium in Mg-Al alloy; $x_{Mg(alloy)}$ is the magnesium molar content in Mg-Al alloy; P^0_{Mg} =1.9atm is the magnesium vapor pressure at T=1175°C; and $P_{Mg(flux)}$ is the partial pressure of magnesium vapor in equilibrium with liquid magnesium dissolved in flux at the cathode, where $P_{Mg(flux)} < 1$atm.

According to Equation (5), the first electrorefining potential and the open circuit voltage depend on the ratio of activity of magnesium dissolved in the flux and the activity of magnesium in the alloy. There is a minor difference between the open circuit voltage and the first electrorefining potential in the experimental measurement caused by the fluctuating value of $P_{Mg(flux)}$.

The second current jump at the higher potential is due to the following reaction:

Anode: $Mg(alloy) \rightarrow Mg^{2+} + 2e^-$ (6)
Cathode: $Mg^{2+} + 2e^- \rightarrow Mg(g)$ (7)

where the overall reaction is:

$$Mg(alloy) \rightarrow Mg(g) \qquad (8)$$

The theoretical expression of electrorefining potential for Equation (8) is given by

$$E_{ER2} = E_{anode} - E_{cathode} = \frac{RT}{2F} \ln \frac{a_{Mg(g)}}{a_{Mg(alloy)}} = \frac{RT}{2F} \ln \frac{P_{Mg(g)}}{\gamma x_{Mg(alloy)} P^0_{Mg}} \qquad (9)$$

and is plotted in Figure 4, where γ is the activity coefficient of magnesium in Mg-Al alloy; $x_{Mg(alloy)}$ is the magnesium molar content in Mg-Al alloy; P_{Mg}^0 =1.9atm is the magnesium saturated vapor pressure at T=1175°C; and $P_{Mg(g)}$=1atm is the magnesium vapor partial pressure at the cathode. The electrorefining potential depends on the ratio of magnesium vapor activity at the cathode and magnesium activity in the alloy.
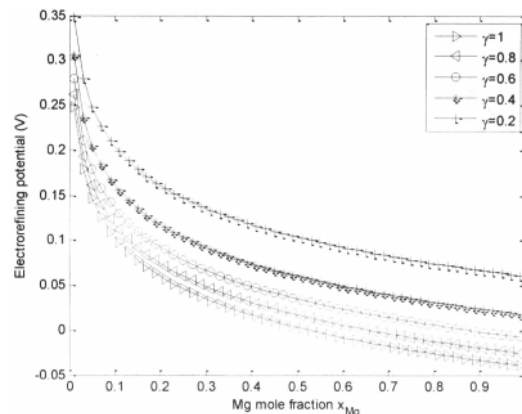

Figure 4. Theoretical values of the second electrorefining potential (based on Equation 9) of magnesium from Mg-Al scrap for different magnesium activity coefficients.

From Figure 4, as the magnesium content in the scrap goes down, the second electrorefining potential increases. The experimental result of the dependence of the second electrorefining potential and the open circuit voltage is shown in Figure 5. The second electrorefining potential and open circuit voltage increase with time, which indicates that the magnesium content in the scrap is decreasing as refining proceeds. The reason why the magnesium content in the scrap decreases is due to the finite solubility of magnesium in the flux. Magnesium dissolution in the flux is followed by vapor phase removal of the dissolved magnesium from the flux. The refining process can be expressed as: $Mg(alloy) \rightarrow Mg(flux) \rightarrow Mg(g)$. Overall, pure magnesium is refined from magnesium scrap.
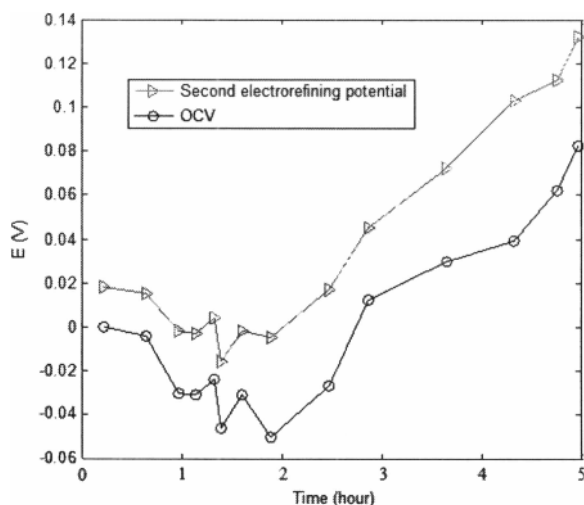

Figure 5. Second electrorefining potential (red triangle) and OCV (black circle) during refining process.

2. SOM electrolysis process

Once the second electrorefining potential reached 0.13V, the anode was switched from the scrap anode to the liquid silver and carbon rod inside the YSZ tube, and a new potential was applied.

When the potential reaches the dissociation potential of magnesium oxide, oxygen ions are pumped out of the flux through the YSZ membrane and are oxidized at the liquid silver anode by the carbon rod; meanwhile, magnesium ions at the cathode are reduced to magnesium metal vapor, which is collected in the condenser.

Electrolysis was performed for a total of two hours at a potential of 3V. The blue curve in Figure 6 shows the initial potentiodynamic scan before any SOM electrolysis was performed, and shows an electronic current of 0.35A due to the dissolution of magnesium from the scrap into the flux. The blue curve in Figure 7 shows the current-time relationship during the first hour of electrolysis. Current efficiency is defined as the ratio of Faradic current to total current, and was calculated to be approximately 41% for the first hour of electrolysis. This is done by measuring the flow rate of carbon monoxide produced from the reaction of the carbon rod and oxygen on the anode side of the YSZ membrane. Based on the volume of carbon monoxide generated, magnesium reduced at the cathode was calculated to be 0.18g during the first hour of SOM electrolysis.

The red curve in Figure 6 shows the potentiodynamic scan before the second hour of SOM electrolysis, which shows the leakage current has increased due to a higher concentration of magnesium dissolved in the flux. The red curve in Figure 7 shows the current-time relationship during the second hour of SOM electrolysis. For the second hour of electrolysis, the current efficiency was 39%, and the amount of magnesium reduced was 0.22g. The total amount of magnesium reduced in the entire two hours of SOM electrolysis process was 0.4g.

The combination of refining and SOM electrolysis processes are shown in the schematic in Figure 8.

Figure 8. Schematic for refining and SOM electrolysis processes.

The total magnesium collected in the condenser from both the refining and SOM processes was weighed to be 7.4g. The Energy-dispersive X-ray spectroscopy (EDS) results for the collected magnesium are shown in Figure 9. The purity of the collected magnesium was determined to be 99.6wt%.
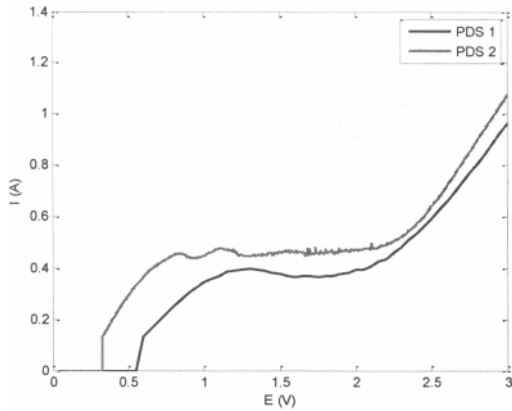

Figure 6. Potentiodynamic scan before the first hour of SOM electrolysis (blue curve) and before the second hour of SOM electrolysis (red curve).

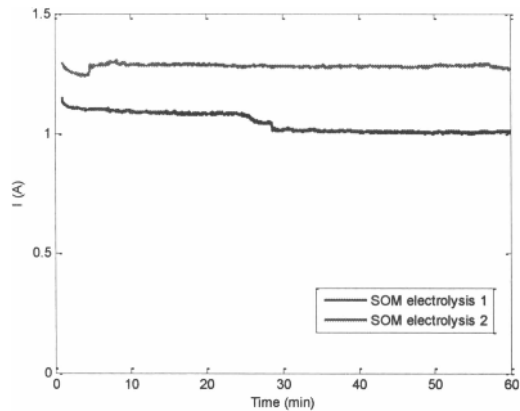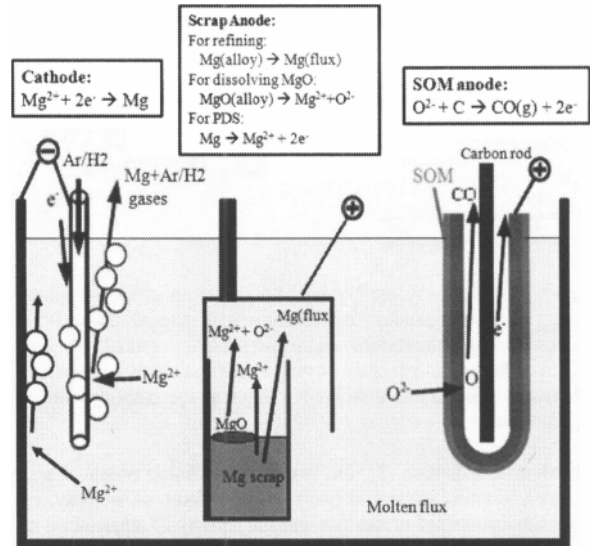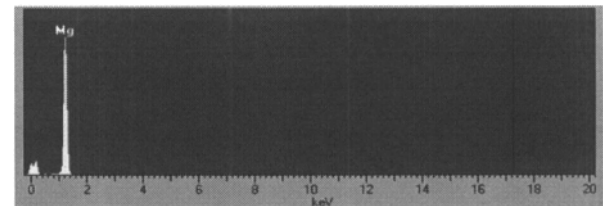Figure 9. EDS results for the collected magnesium.

Figure 7. Current-time relationships for the first hour of electrolysis (blue curve) and the second hour of electrolysis (red curve). Both electrolyses were performed at 3V.
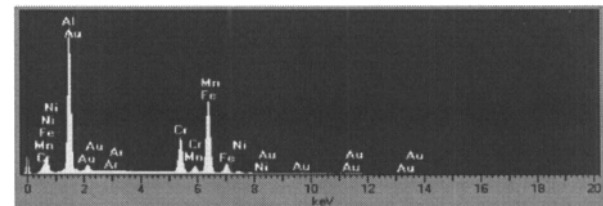
Figure 10. EDS results for the scrap residue inside the alloy crucible.

The scrap residue remained at the bottom of the alloy crucible. The iron powder and iron and chromium from the SS 304 crucibles alloyed with the scrap, which has a density higher than the flux. EDS was performed for the magnesium residue, and the results are shown in Figure 10. Only trace magnesium remains in the alloy, thus approximately 100% of the magnesium has been refined. Future experiments are also planned wherein the stainless steel parts will be replaced by low carbon steel to minimize additional dissolution of elements (Cr, Ni and Mn).

Conclusions

The combination of the novel refining process and the SOM electrolysis process for recycling magnesium from magnesium scrap was carried out, and yielded 7.4g of pure magnesium metal. A small amount of magnesium condensed on the walls of the condenser and dissolved in the 680g of flux, and could not be quantified. No measurable amount of magnesium remained in the magnesium scrap, which implies that the refining efficiency is almost 100% using this novel refining process of dissolving magnesium and its oxide from the scrap into the flux, followed by vapor phase removal of dissolved magnesium. After the refining process, the SOM electrolysis process was employed in the refining system to enable the recycling of an additional 0.4g magnesium from magnesium oxide in both the scrap and the flux. This paper presented the technical feasibility of recycling magnesium from partially oxidized Mg-Al alloy by the combination of refining and SOM electrolysis processes. In the future, this approach will be tested using larger amounts of oxidized scrap with additional impurities and less initial oxide content in the flux.

Acknowledgements

References

[1] United States Automotive Materials Partnership (USAMP), *Magnesium Vision 2020: A North American Automotive Strategic Vision for Magnesium*, Technical Report, USCAR, November 2006.

[2] J. F. Kurgan, "Electromagnetic shield for electrical circuit," *US patent 5053924*, 1 October 1991.

[3] W. O, R. JB, "Method and apparatus for remelting and refining of magnesium and magnesium alloys," *US Patent 5167700*, 1 December 1992.

[4] H. E. Friedrich, B. L. Mordike, *Magnesium Technology: metallurgy, design data, applications* (Springer, 2006), 638.

[5] S. D. Cramer and B. S. Covino, *ASM Handbook, Volume 13A: Corrosion: Fundamentals, Testing, and Protection* (ASM international, 2003), 693.

[6] T. Zhu et al., "Innovative vacuum distillation for magnesium recycling", *Magnesium Technology 2001* (TMS, 2001), 55-60.

[7] G. Hanko, H. Antrekowitsch and P. Ebner, "Recycling automotive magnesium scrap," *Journal of the Minerals, Metals and Materials society*, 54 (2) (2002) 51-54.

[8] P. Chartrand and A. D. Pelton, "Thermodynamic evaluation and optimization of the LiF-NaF-KF-MgF$_2$-CaF$_2$ system using the modified quasi-chemical model," *Metallurgical and Materials Transactions A*, 32 (6) (2001) 1385-1396.

[9] A. Krishnan, U. B. Pal and X. G. Lu, "Solid Oxide Membrane Process for Magnesium Production Directly from Magnesium Oxide," *Metallurgical and Materials Transaction B*, 36 (4) (2005), 463-473.

[10] U. B. Pal, A. C. Powell, "The Use of Solid-oxide-membrane Technology for Electrometallurgy," *Journal of the Minerals, Metals and Materials Society*, 59 (5) (2007), 44-49.

[11] J. Wypartowicz, T. Ostvold and H. Oye, "The Solubility of Magnesium Metal and the Recombination Reaction in the Industrial Magnesium Electrolysis," *Electrochimica ACTA*, 25 (1980), 151-156.

[12] E. Gratz et al., "Efficiency and Stability of Solid Oxide Membrane Electrolyzers for Magnesium Production," *Magnesium Technology 2011* (Wiley-TMS, 2011), 39-42.